International Journal of Thermal Sciences 48 (2009) 2053–2062

Contents lists available at ScienceDirect

International Journal of Thermal Sciences

journal homepage: www.elsevier.com/locate/ijts

Thermal wave oscillations and thermal relaxation time determination in a hyperbolic heat transport model

J. Ordóñez-Miranda, J.J. Alvarado-Gil*

Applied Physics Department, Centro de Investigación y de Estudios Avanzados del I.P.N-Unidad Mérida. Carretera Antigua a Progreso km. 6, A.P. 73 Cordemex, Mérida 97310, Yucatán, Mexico

ARTICLE INFO

Article history:
Received 2 December 2008
Received in revised form
6 March 2009
Accepted 7 March 2009
Available online 11 April 2009

Keywords:
Thermal relaxation time
Thermal wave oscillations
Hyperbolic heat transfer
Cattaneo–Vernotte heat conduction equation
Two-layer system

ABSTRACT

One of the major challenges in the study of thermal transport and its analysis, based on the hyperbolic model associated with Cattaneo equation, is the fact that it is necessary to determine the thermal relaxation time for the analyzed materials. This parameter has been an elusive physical quantity to be determined experimentally even though it is of crucial importance in heat transport. In this paper a system formed by a semi-infinite layer in contact with a finite one, that is excited by a modulated heat source is studied. It is shown that a frequency range can be found in which the amplitude and phase of the spatial component of the oscillatory surface temperature show strong oscillations when the thermal relaxation time of the finite layer is close to its thermalization time. When the thermal effusivities of the layers are quite different or their thermal relaxation times are similar, it is shown that simple analytical expressions for the values of the maxima and minima of the oscillations as well as for the frequencies, at which they occur, are obtained. These results were used to establish a methodology to determine the thermal relaxation time as well as additional thermal properties of the finite layer.

1. Introduction

Heat transport has been traditionally studied based on Fourier law, which is supported by an impressive quantity of useful and successful results showing very good agreement with experimental data for most of the analyzed experimental conditions [1,2].

However, it is well known that Fourier heat diffusion law predicts an infinite velocity for heat propagation, in such a way that a temperature change in any part of the material results in an instantaneous perturbation at each point of the sample [3,6]. The origin of this fundamental problem is due to the fact that Fourier law establishes that, when a temperature gradient at time t is imposed, the heat flux starts instantaneously at the same time t. Considering that heat transport is due to microscopic motion and collisions of electrons and phonons, it can be inferred that the Fourier condition on the velocity of heat transport cannot be sustained [3–8].

One of the most simple and accepted approaches that surmounts the limitation of Fourier law [3,4], was suggested by Cattaneo [9] and independently by Vernotte [10]. It consists of modifying the heat flux equation, incorporating the finite propagation speed of heat. The one-dimensional form of Cattaneo–Vernotte equation is,

$$J(x,t+\tau) = -k\frac{\partial T(x,t)}{\partial x}, \tag{1}$$

where t is the time, x is the spatial coordinate, J [W/m^2] is the heat flux, T (K) is the absolute temperature, k [W/m K] is the thermal conductivity and τ(s) is the thermal relaxation time, which represents the time necessary for the initiation of the heat flux after a temperature gradient has been imposed. Eq. (1) establishes that the heat flux does not start instantaneously, but rather grows gradually, depending on the thermal relaxation time, after the application of the temperature gradient [3].

From Eq. (1), expanding the heat flux in Taylor series around $\tau = 0$, and approximating at first order in τ,

$$J(x,t) + \tau\frac{\partial J(x,t)}{\partial t} = -k\frac{\partial T(x,t)}{\partial x}. \tag{2}$$

On the other hand, energy conservation equation is given by [1]

$$\frac{\partial J(x,t)}{\partial x} + \rho c\frac{\partial T(x,t)}{\partial t} = S(x,t), \tag{3}$$

where ρ [kg/m^3] is the density, c [J/kg K] is the specific heat of the medium and the source term S [W/m^3] represents the rate per unit

* Corresponding author. Tel.: +52 999 9429421; fax: + 52 999 9812917.
E-mail addresses: eordonez@mda.cinvestav.mx (J. Ordóñez-Miranda), jjag@mda.cinvestav.mx (J.J. Alvarado-Gil).

1290-0729/$ – see front matter © 2009 Elsevier Masson SAS. All rights reserved.
doi:10.1016/j.ijthermalsci.2009.03.008

Nomenclature

a	non-dimensional constant
A	amplitude of the spatial part of the oscillatory surface temperature
c	specific heat
f	frequency
F	time-independent factor of the heat source
I	light beam intensity
J	heat flux
k	thermal conductivity
l	thickness of the first layer
q	complex wave number
Re()	real part
S	heat source
t	time
T	temperature
x	spatial coordinate
X	non-dimensional parameter

Greek symbols

α	thermal diffusivity
Δ	difference
ε	thermal effusivity
θ	spatial part of the oscillatory temperature
λ	complex parameter
μ	classical thermal diffusion length
ρ	density
τ	thermal relaxation time
ϕ	phase of the spatial part of the oscillatory surface temperature
χ	real parameter
ω	angular frequency
Ω	ratio of the maximum to minimum amplitude, A_{max}/A_{min}

Subscripts

ac	relative to the time-dependent temperature
amb	ambient
dc	relative to a time-independent temperature
m	thermalization
max	maximum value
min	minimum value
0	relative to the semi-infinite layer
n	natural number
01	relative to the ratio of thermal effusivities

Superscripts

(0)	relative to the term of X, independent of the thermal relaxation time.

volume at which the heat flux is generated. Combining Eqs. (2) and (3), the hyperbolic Cattaneo–Vernotte heat conduction equation is obtained [3,9–11]:

$$\frac{\partial^2 T(x,t)}{\partial x^2}-\frac{1}{\alpha}\frac{\partial T(x,t)}{\partial t}-\frac{\tau}{\alpha}\frac{\partial^2 T(x,t)}{\partial t^2}=-\frac{1}{k}\left(S(x,t)+\tau\frac{\partial S(x,t)}{\partial t}\right), \tag{4}$$

where α [m^2/s] is the thermal diffusivity of the material [12]. On the left hand side of this equation, the second order time derivative term indicates that heat propagates as a wave with a characteristic speed $\sqrt{\alpha/\tau}$ and the first order time derivative corresponds to a diffusive process, which damps spatially the heat wave. Eq. (4) reduces to the parabolic heat conduction equation (based on Fourier law) for $\tau=0$ or in steady-state conditions $\partial J(x,t)/\partial t=0$ [3,13].

Thermal relaxation time is associated with the average communication time among the collisions of electrons and phonons [3], and it has been theoretically estimated for metals, superconductors and semiconductors to be of the order of microseconds (10^{-6} s) to picoseconds (10^{-12} s) [11,14,15]. These small values of the thermal relaxation time indicate that its effects will not be significant if the physical time scales are of the order of microseconds or larger. In these situations Fourier law provides an adequate approach. However, in modern applications such as in analysis and processing of materials using ultrashort laser pulses and high speed electronic devices, the finite value of the thermal relaxation time should be considered [13–18].

The measurement of the thermal relaxation time and the subsequent hyperbolic effects in heat transport have been elusive problems [15,19]. In fact there are research groups indicating that hyperbolic effects can be easily observed, and that they are associated with thermal relaxation times of the orders of seconds in materials with non-homogeneous structure [16–18]. In contrast, other authors have criticized their experimental methodologies and have suggested alternative experimental arrangements; obtaining results that do not seem to be affected by hyperbolic effects [20,21]. Therefore, in this last case, if Cattaneo equation is considered adequate, it would indicate that the observed results would be associated with very short thermal relaxation times [20]. More careful experiments, using a modulated heat source, for similar materials, have shown that in order to determine the thermal relaxation time, it is important to measure simultaneously the thermal diffusivity, also using a hyperbolic approach [18]. In this context, Roetzel et al. [18] have found hyperbolic effects, associated with thermal relaxation times of at least one order of magnitude smaller when compared with the results of Kaminski [16] and Mitra et al. [17]. In the experiments reported by Roetzel et al., the methodology is based on a phase lag method, however given that this is a feature that is also present in the parabolic approach, it is not easy to accept or reject the possibility of a hyperbolic behavior. It has also been shown that the thermal diffusivity and thermal relaxation time can be determined from the thermal profiles; however the suggested methodology makes difficult the accurate determination of these parameters, due to the fact that a small change in the thermal diffusivity can result in a large change in the thermal relaxation time [18].

It is of the main importance to develop a methodology to establish when without a doubt hyperbolic effects are being observed and how from these results, a measurement of the thermal relaxation time can be obtained. For steady-state boundary conditions, a comprehensive discussion of both the hyperbolic effects and the methods for the measurement of the thermal relaxation time have already been presented in the recent book by Wang, Zhou and Wei [19] and in the articles of Mengi and Turhan [22], and Tan and Yang [23]. Otherwise, for modulated heat sources, it could be expected that the advantages found in photothermal science in the analysis of thermal depth profiles using Fourier equation can also arise when the same kind of heat sources is used with hyperbolic Cattaneo–Vernotte equation [11].

In this paper, heat transport governed by Cattaneo–Vernotte equation in a system formed by a finite layer in perfect thermal contact [24] with a semi-infinite layer of a different material is analyzed when

the first layer is excited with a periodic source. It is shown that, when the thermal relaxation time of the finite layer is near to its thermalization time, it is possible to find a frequency range, at which the temperature at both sides of the finite layer shows an evident hyperbolic behavior, depending on the boundary conditions. In such conditions, oscillations of the spatial component of the surface temperature as a function of the modulation frequency are obtained.

When the thermal effusivities of the layers are quite different or when the thermal relaxation times of both layers are similar, it is shown that analytical expressions for the values of the maxima and minima as well as the frequencies at which they occur, can be obtained. From these results, the thermal relaxation time can be determined. It is also shown that depending on the ratio of thermal effusivities of the layers and the boundary conditions, the thermal properties of the finite layer can be determined simultaneously.

2. Formulation of the problem and solutions

Let us consider the configuration shown in Fig. 1, in which the system is excited at the surface $x = 0$, with a modulated heat source at frequency f, of the form [11,25]:

$$S(x,t) = F(x)(1+\cos(\omega t)) = \mathrm{Re}\left[F(x)\left(1+\mathrm{e}^{\mathrm{i}\omega t}\right)\right], \tag{5}$$

where $\omega = 2\pi f$, $\mathrm{Re}(\xi)$ is the real part of ξ and F [W/m^3] is the spatial distribution of deposited energy over the sample per unit volume and unit time. The temperature at any point of the sample is given by:

$$T(x,t) = T_{\mathrm{amb}} + T_{\mathrm{dc}}(x) + T_{\mathrm{ac}}(x,t), \tag{6}$$

where T_{amb} corresponds to the ambient temperature, $T_{\mathrm{dc}}(x)$ and $T_{\mathrm{dc}}(x,t) = \mathrm{Re}|\theta(x)\mathrm{e}^{\mathrm{i}wt}|$ are the stationary raising and periodic components of the temperature, these last two terms are due to the first and second terms of the heat source, respectively. From now on, the operator Re() will be omitted, taking into account the convention that the real part of the expressions of the temperature must be taken to obtain physical quantities. Our attention will be focused on the spatial component $[\theta(x)]$ of the oscillatory part of the temperature, due to the fact that it is the quantity of interest in lock-in and similar detection techniques.

Inserting Eqs. (5) and (6) into Eq. (4) and considering that there are not any internal heat sources, then for $x > 0$, the general solution of Eq. (4) for $\theta = (x)$ is given by:

$$\theta(x) = B\mathrm{e}^{qx} + C\mathrm{e}^{-qx}, \tag{7}$$

where B and C are two constants that depend on the boundary conditions of the particular problem and q is given by:

$$q = \sqrt{\frac{\mathrm{i}\omega}{\alpha}}\sqrt{1+\mathrm{i}\omega\tau} = \frac{\chi + \mathrm{i}\chi^{-1}}{\mu}, \tag{8a}$$

$$\mu = \sqrt{\frac{2\alpha}{\omega}} = \sqrt{\frac{\alpha}{\pi f}}, \tag{8b}$$

$$\chi = \sqrt{\sqrt{1+(\omega\tau)^2} - \omega\tau}. \tag{8c}$$

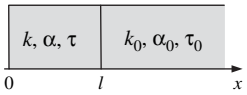

Fig. 1. Schematic diagram of the analyzed system, with k, α, τ and k_0, α_0, τ_0 being the thermal conductivity, thermal diffusivity and thermal relaxation time of the finite and semi-infinite layers respectively. The excitation heat source is applied at $x = 0$.

Assuming that the layers are in perfect thermal contact, that is to say, there are not any interface thermal resistance between them [1,24,26], the boundary conditions obtained from the usual requirement of temperature and heat flux continuity at the interface $x = l$, are given by:

$$\theta\left(x^-\right) = \theta\left(x^+\right), \tag{9a}$$

$$\frac{k(x^-)}{1+\mathrm{i}\omega\tau^-}\frac{\mathrm{d}\theta(x^-)}{\mathrm{d}x} = \frac{k(x^+)}{1+\mathrm{i}\omega\tau^+}\frac{\mathrm{d}\theta(x^+)}{\mathrm{d}x}, \tag{9b}$$

where the superscripts "+" and "−" indicate that the limit $x \to l$ is taken from the right and left of the point $x = l$, respectively. From now on, two types of modulated heat sources are considered, the first one specifying the temperature and the second one the heat flux, in both cases, at the surface $x = 0$.

2.1. Dirichlet problem

In this case the following boundary condition is considered:

$$\theta(x = 0) = \theta_0, \tag{10}$$

where θ_0 is a positive non-zero constant. From Eqs. (7), (9) and (10), the solution for the spatial part of the thermal wave at $x = l$, is given by:

$$\theta(l) = \frac{2\theta_0}{(1+\lambda)\mathrm{e}^{ql} + (1-\lambda)\mathrm{e}^{-ql}}, \tag{11}$$

where q is defined by Eq. (8a) for the thermal properties of the finite layer and $\lambda = (\varepsilon_0/\varepsilon)\sqrt{(1+\mathrm{i}\omega\tau)/(1+\mathrm{i}\omega\tau_0)}$, being $\varepsilon = k/\sqrt{\alpha}$, the thermal effusivity of the finite layer and ε_0 the corresponding one of the semi-infinite layer.

2.2. Neumann problem

Considering that the surface $x = 0$ is excited by a periodic heat flux, this situation can be fulfilled when the opaque surface of a material is uniformly illuminated by a laser light beam of periodically modulated intensity. In this case the heat source is given by [11,27]:

$$I_0[1+\cos(\omega t)]/2 = \mathrm{Re}\left[I_0\left(1+\mathrm{e}^{\mathrm{i}\omega t}\right)/2\right],$$

where the $I_0 = F\eta(1-R)I$, F being a parameter determined by the optical, thermal and geometric properties of the first layer, η the efficiency at which the absorbed light is converted into heat, R is the reflection coefficient of the surface at $x = 0$ and I [W/m^2] is the intensity of the light beam [11,27,28]. Considering that the sample is uniformly illuminated with a fixed light source the factor I_0 can be taken as nearly constant and independent of the modulation frequency as it is usually assumed in similar problems [11,28]. The boundary condition in this case has the following form:

$$-\frac{k}{1+\mathrm{i}\omega\tau}\left.\frac{\mathrm{d}\theta(x)}{\mathrm{d}x}\right|_{x=0} = \frac{I_0}{2}. \tag{12}$$

From Eqs. (7), (9) and (12), the solution for the spatial part of the thermal wave at $x = 0$, is given by:

$$\theta(0) = \frac{I_0}{2}\frac{1+\mathrm{i}\omega\tau}{kq}\frac{(1+\lambda)\mathrm{e}^{ql} + (1-\lambda)\mathrm{e}^{-ql}}{(1+\lambda)\mathrm{e}^{ql} - (1-\lambda)\mathrm{e}^{-ql}}, \tag{13}$$

and for $x = l$, it is obtained:

$$\theta(l) = \frac{I_0}{2}\frac{1+\mathrm{i}\omega\tau}{kq}\frac{2}{(1+\lambda)\mathrm{e}^{ql}-(1-\lambda)\mathrm{e}^{-ql}}. \tag{14}$$

Expressing $\theta(x=0,l)$ as a complex function in its polar form, both its amplitude $A(f)$ and phase $\phi(f)$, can be obtained at $x=0,l$ respectively. Final expressions are long and complicated, however when the ratio of the thermal effusivities of the layers is quite different from the unit or when their thermal relaxation times are similar, useful expressions for the determination of the thermal properties can be found.

3. Analysis and discussions

The analysis of the thermal profiles is performed at $x=l$ for the Dirichlet boundary condition and at $x=0$ and $x=l$ for the Neumann boundary condition.

3.1. Dirichlet problem

3.1.1. Semi-infinite layer thermal effusivity much lower than the one of the finite layer: $\varepsilon_0/\varepsilon=0$

An approximate example of this case is given by a metallic layer of high thermal effusivity in contact with an air layer acting as the semi-infinite medium [27]. From Eq. (11), the results for the amplitude and phase reduce to:

$$A(f) = \frac{\theta_0}{\sqrt{\sinh^2\left(\frac{l\chi}{\mu}\right)+\cos^2\left(\frac{l}{\mu\chi}\right)}}, \tag{15a}$$

$$\phi(f) = -\frac{l}{\mu\chi}+\arctan\left[\frac{\sin\left(\frac{2l}{\mu\chi}\right)}{\mathrm{e}^{\frac{2l\chi}{\mu}}+\cos\left(\frac{2l}{\mu\chi}\right)}\right], \tag{15b}$$

where μ and χ are defined by Eqs. (8b) and (8c) for the thermal properties of the first layer.

The normalized amplitude and phase as a function of the modulation frequency are shown in Fig. 2(a) and (b), respectively; for three values of the thermal relaxation time of the first layer $\tau=5\times10^{-7}$ s, 9×10^{-7} s which are characteristic of crystal semiconductors [14]. The thickness of the finite layer is $l=20$ μm and its thermal diffusivity is $\alpha=5\times10^{-5}$ m^2/s, from which it is obtained that the thermalization time ($\tau_\mathrm{m}=l^2/4\alpha$) [29,30] of the first layer is $\tau_\mathrm{m}=2\times10^{-6}$ s. The corresponding amplitude and phase predicted by the Fourier parabolic approach ($\tau=0$) are shown in the same figures by dashed lines.

In Fig. 2(a) it is shown that the parabolic amplitude presents the typical behavior of traditional thermal wave phenomena based on Fourier equation, in which a strong attenuation of the temperature, when the frequency increases, is observed [2,31]. In contrast, when τ becomes closer to the thermalization time, heat transport enhances, which is a characteristic of hyperbolic behavior, due to the second order time derivative [Eq. (4)]. It can be observed that for low frequencies ($\omega\tau=2\pi f\ll1$), the behavior of the amplitudes predicted by the parabolic and hyperbolic models is similar, in contrast for higher frequencies ($\omega\tau\gg1$), where the hyperbolic effects are dominant, the hyperbolic model predicts an oscillatory amplitude.

For a first order approximation in $(\omega\tau)^{-1}$ Eq. (15a) can be simplified to,

$$A(f) = \frac{\theta_0}{\sqrt{\sinh^2(a/2)+\cos^2(\omega\tau a)}}, \tag{16}$$

where $a = l/\sqrt{\alpha\tau}$. Looking at the oscillatory term in Eq. (16), it can be inferred that the amplitude $A(f)$ has maxima and minima given by,

$$A_\mathrm{max} = \frac{\theta_0}{\sinh(a/2)}, \tag{17a}$$

$$A_\mathrm{min} = \frac{\theta_0}{\cosh(a/2)}, \tag{17b}$$

which occurs at the following modulation frequencies

$$f_n = \frac{1}{2l}\sqrt{\frac{\alpha}{\tau}}\begin{cases} n+\frac{1}{2}, & A=A_\mathrm{max},\\ n, & A=A_\mathrm{min},\end{cases} \tag{18}$$

where $f_n=\omega_n/2\pi$, $n=1,2,3,\ldots$.

The measurement of the maximum and minimum values of the amplitude as well as the frequencies at which they occur would allow to establish a methodology to determine the thermal relaxation time τ of a layer of thickness l and known thermal diffusivity a using Eqs. (17) and (18), as follows:

- Method 1. – Measuring the value of the frequency for which the amplitude has a maximum or minimum and using Eq. (18) to determine τ.

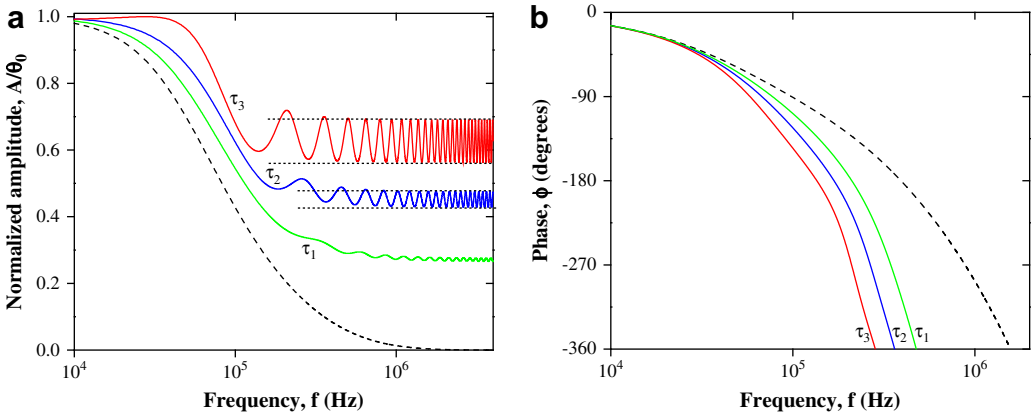

Fig. 2. Frequency dependence at $x=l$ of the (a) normalized amplitude and (b) phase of the temperature, for Dirichlet problem, when $\varepsilon_0/\varepsilon=0$. The dashed line corresponds to the parabolic model and the solid lines to the hyperbolic one for three values of τ:$\tau_1=5\times10^{-7}$ s, $\tau_2=9\times10^{-7}$ s and $\tau_3=1.5\times10^{-6}$ s.

■ Method 2. – Measuring the value of a maximum or minimum of the amplitude and using Eqs. (17) to determine $\tau(a = 1/\sqrt{\alpha\tau})$.

In Fig. 2(a) the horizontal dotted lines follow the maximum and minimum values of the amplitude predicted by Eqs. (17a) and (17b). It can be observed that the first two peaks or valleys are not well predicted by these equations and therefore in Method 1 or 2, it is necessary to use $n = 3$ or higher values of n, for which the prediction improves.

In Fig. 2(b), the phase spectrum of the temperature at $x = l$ is shown. It can be observed that the phase does not present an oscillatory behavior, and even though it could be used to determine the thermal diffusivity or thermal relaxation time [18], it would imply a different and probably less sensitive methodology than the one presented in this work.

3.1.2. Semi-infinite layer thermal effusivity much higher than the one of the finite layer: $\varepsilon_0/\varepsilon \to \infty$

An approximate example of this case is given by a copper layer acting as the semi-infinite one and the first layer being made of glass. In this case the contribution to the temperature given by Eq. (11) vanishes and therefore it cannot be used to determine the thermal relaxation time.

3.1.3. Semi-infinite and finite layers with close thermal relaxation times: $\tau_0 = \tau + \Delta\tau$

An example of this case is given by a metallic layer acting as the first one and an alloy of the same metal as the semi-infinite layer [25]. Considering that $|\Delta\tau|/\tau$ and $\omega\tau \gg 1$, for a first order approximation in $|\Delta\tau|/\tau$ and $(\omega\tau)^{-1}$, the amplitude of the temperature obtained from Eq. (11) is,

$$A(f) = \frac{\theta_0(1+X)}{\sqrt{\left(e^{a/2}+Xe^{-a/2}\right)^2 - 4X\sin^2(\omega\tau a)}}, \tag{19}$$

where,

$$\begin{cases} X = X^{(0)} + \dfrac{\Delta\tau}{\tau}\dfrac{\varepsilon_{01}}{(1+\varepsilon_{01})^2}, \\ X^{(0)} = \dfrac{1-\varepsilon_{01}}{1+\varepsilon_{01}}, \\ \varepsilon_{01} = \varepsilon_0/\varepsilon, \\ a = l/\sqrt{\alpha\tau}. \end{cases} \tag{20}$$

The normalized amplitude of the temperature as a function of the modulation frequency is shown in Fig. 3, for two values of the thermal relaxation time of the first layer (τ:$\tau_1 = 9\times10^{-7}$ s and $\tau_2 = 1.5\times10^{-6}$ s) and for the case in which $\varepsilon_0/\varepsilon = 0$ and $\Delta\tau = 5\times10^{-8}$ s. The corresponding amplitude predicted by the parabolic model ($\tau = 0$) is shown in the same figure by dashed line.

The behavior of the amplitude predicted by the hyperbolic model reduces to the one predicted by the parabolic model for $\omega\tau \ll 1$. When $\omega\tau \gg 1$, the parabolic amplitude falls down to zero rapidly when the frequency increases. In contrast, in the hyperbolic model the amplitude oscillates around a constant value with frequency independent maxima and minima.

Similarly to the case in which $\varepsilon_0/\varepsilon = 0$ [See Fig. 2(b)], the phase of the temperature does not present an oscillatory behavior and therefore it is not going to be analyzed.

The values of the maxima and minima of the temperature amplitude are given by:

$$A_{\max} = \frac{\theta_0(1+X)}{e^{a/2}-Xe^{-a/2}}, \tag{21a}$$

$$A_{\min} = \frac{\theta_0(1+X)}{e^{a/2}+Xe^{-a/2}}, \tag{21b}$$

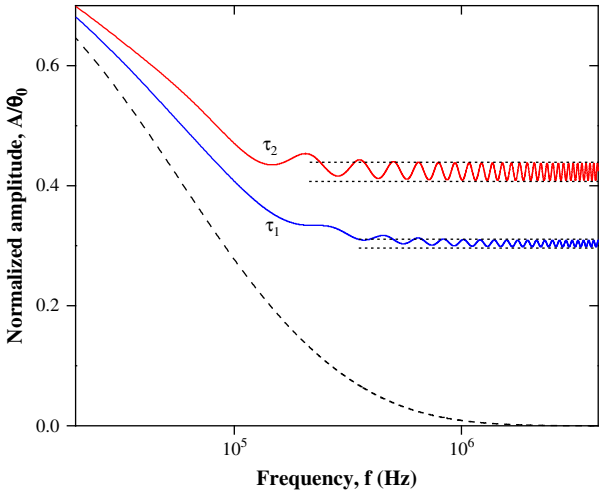

Fig. 3. Normalized amplitude of the temperature at $x = l$, for Dirichlet problem, when $\tau_0 = \tau + \Delta\tau$. The dashed line corresponds to the parabolic model ($\tau = 0$) and the solid lines to the hyperbolic one for two values of τ:$\tau_1 = 9\times10^{-7}$ s and $\tau_2 = 1.5\times10^{-6}$ s, with $\varepsilon_0/\varepsilon = 0.5$ and $\Delta\tau = 5\times10^{-8}$ s.

where we have assumed that $X > 0$. These extreme values of the amplitude [Eqs. (21a) and (21b)] occur at the frequencies given by Eq. (18), which can be used to measure the thermal relaxation time τ, with Method 1, previously explained.

Solving Eqs. (21a) and (21b) for X, it is obtained:

$$X = \begin{cases} \dfrac{a_{\max}e^{a/2}-1}{a_{\max}e^{-a/2}+1}, & a_{\max} = \dfrac{A_{\max}}{\theta_0}, \\ -\dfrac{a_{\min}e^{a/2}-1}{a_{\min}e^{-a/2}+1}, & a_{\min} = \dfrac{A_{\min}}{\theta_0}. \end{cases} \tag{22}$$

After having calculated τ and therefore the value of $a = 1/\sqrt{\alpha\tau}$, X can be determined using Eq. (22) and finally with Eq. (20), the value of $\Delta\tau$ can be measured, when $\varepsilon_0/\varepsilon$ is known.

It is important to keep in mind that Eqs. (21) and (22) are only valid for the case in which $X > 0$ which is not known until its calculation is performed with Eq. (22). This problem may be surmounted, if at the beginning, it is supposed that $X > 0$ and then checking its validity with Eq. (22). If it is true, our starting supposition is right and the value of X can be used to determine $\Delta\tau$, otherwise the labels "max" and "min" in Eq. (22) must be interchanged and the calculations have to be remade.

Note that these calculations are based on a first order approximation in $\Delta\tau/\tau$. For a higher order approximation, it is also possible to obtain analytical expressions but they are much more complicated than the ones presented here.

3.2. Neumann problem

3.2.1. Semi-infinite layer thermal effusivity much lower than the one of the finite layer: $\varepsilon_0/\varepsilon = 0$

In this case, both the amplitude and phase of $\theta(0)$ given by Eq. (13), reduce to:

$$A(f) = \frac{I_0}{2\varepsilon}\frac{\sqrt[4]{1+(\omega\tau)^2}}{\sqrt{\omega}}\sqrt{\frac{\sinh^2\left(\frac{l\chi}{\mu}\right)+\cos^2\left(\frac{l}{\mu\chi}\right)}{\sinh^2\left(\frac{l\chi}{\mu}\right)+\sin^2\left(\frac{l}{\mu\chi}\right)}}, \tag{23}$$

$$\phi(f) = -\frac{\pi}{4}+\frac{1}{2}\arctan(\omega\tau)-\arctan\left[\frac{\sin\left(\frac{2l}{\mu\chi}\right)}{\sinh\left(\frac{2l\chi}{\mu}\right)}\right]. \tag{24}$$

If $\omega \to 0$ the amplitude of the temperature diverges and the phase tends to $-\pi/2$, the normalized amplitude $[A(f)2\varepsilon/I_0]$ and phase as a function of the modulation frequency are shown in Fig. 4(a) and (b), taking $l = 20\,\mu\text{m}$ and $\alpha = 5\times10^{-5}\,\text{m}^2/\text{s}$ for two values of τ ($\tau = 8\times10^{-7}$ s and 1.5×10^{-6} s) which are characteristic of crystal semiconductors [14]. The dashed lines represent the amplitude and phase corresponding to the parabolic model, which shows a strong attenuation of the thermal waves, generated by a heat flux, when the frequency increases [31,32]. In contrast for higher values of the thermal relaxation time of the first layer, close to its thermalization time ($\tau = 2\times10^{-6}$ s), the heat transport enhances showing oscillations in amplitude and phase at high frequencies ($\omega\tau \gg 1$). For a first order approximation in $(\omega\tau)^{-1}$, the amplitude given in Eq. (23) reduces to:

$$A(f) = \frac{I_0\sqrt{\tau}}{2\varepsilon}\sqrt{\frac{\sinh^2(a/2)+\cos^2(\omega\tau a)}{\sinh^2(a/2)+\sin^2(\omega\tau a)}}, \tag{25}$$

where $a = l/\sqrt{\alpha\tau}$. Analyzing the oscillatory terms in Eq. (25), it can be found that the maxima and minima of the amplitude of the temperature are given by,

$$A_{\max} = \frac{I_0\sqrt{\tau}}{2\varepsilon}\sqrt{\frac{\sinh^2(a/2)+1}{\sinh^2(a/2)}} = \frac{I_0\sqrt{\tau}}{2\varepsilon}\coth(a/2), \tag{26a}$$

$$A_{\min} = \frac{I_0\sqrt{\tau}}{2\varepsilon}\sqrt{\frac{\sinh^2(a/2)}{\sinh^2(a/2)+1}} = \frac{I_0\sqrt{\tau}}{2\varepsilon}\tanh(a/2), \tag{26b}$$

which occur at the frequencies given in Eq. (18), but the labels "max" and "min" must be interchanged.

Using the expression of the phase [Eq. (24)], for a first order approximation in $(\omega\tau)^{-1}$, it is obtained that,

$$\phi(f) = -\frac{\pi}{4}+\frac{1}{2}\arctan(\omega\tau)-\arctan\left[\frac{\sin(2\omega\tau a)}{\sinh(a)}\right]. \tag{27}$$

The maxima and minima of the phase appear when $\sin(2\omega\tau a) = -1$ and $\sin(2\omega\tau a) = +1$, therefore at frequencies,

$$f_n = \frac{1}{2l}\sqrt{\frac{\alpha}{\tau}}\begin{cases} n-\frac{1}{4}, & \phi = \phi_{\max}, \\ n+\frac{1}{4}, & \phi = \phi_{\min}, \end{cases} \tag{28}$$

and are given by,

$$\phi_{\max}(n) = -\frac{\pi}{4}+\frac{1}{2}\arctan\left[\left(n-\frac{1}{4}\right)\frac{\pi}{4}\right]+\arctan\left[\frac{1}{\sinh(a)}\right], \tag{29a}$$

$$\phi_{\min}(n) = -\frac{\pi}{4}+\frac{1}{2}\arctan\left[\left(n+\frac{1}{4}\right)\frac{\pi}{4}\right]-\arctan\left[\frac{1}{\sinh(a)}\right], \tag{29b}$$

with $n = 1,2,3,\ldots$. Interchanging the labels "max" and "min" in Eq. (18), it can be seen that the maxima and minima of the phase [Eqs. (29a) and (29b)] are shifted by a constant quantity $[(1/2l)\sqrt{\alpha/\tau}]/4$, with respect to the corresponding frequencies of the maxima and minima of the amplitude [Eqs. (26a) and (26b)]. Finally, the thermal relaxation time τ can be determined using Eq. (18) or (28) with Method 1 or with Eq. (26) or (29) with the Method 2, for the phase.

3.2.2. Semi-infinite layer with thermal effusivity much higher than the one of finite layer: $\varepsilon_0/\varepsilon \to \infty$

In this case, both the amplitude and phase of the temperature $\theta(0)$ given by Eq. (13) reduce to the following form:

$$A(f) = \frac{I_0}{2\varepsilon}\frac{\sqrt[4]{1+(\omega\tau)^2}}{\sqrt{\omega}}\sqrt{\frac{\sinh^2\left(\frac{l\chi}{\mu}\right)+\sin^2\left(\frac{l}{\mu\chi}\right)}{\sinh^2\left(\frac{l\chi}{\mu}\right)+\cos^2\left(\frac{l}{\mu\chi}\right)}}, \tag{30}$$

$$\phi(f) = -\frac{\pi}{4}+\frac{1}{2}\arctan(\omega\tau)+\arctan\left[\frac{\sin\left(\frac{2l}{\mu\chi}\right)}{\sinh\left(\frac{2l\chi}{\mu}\right)}\right]. \tag{31}$$

In this case, for $\omega \to 0$ the amplitude tends to be $I_0 l/2\sqrt{2}k$ while the phase vanishes. The normalized amplitude and phase as a function of the modulation frequency are shown in Fig. 5(a) and (b) respectively, for the same parameters used in Fig. 4(a). The dashed lines represent the corresponding predictions of the parabolic model, which as it is usual, shows a strong attenuation when the frequency increases. If the thermal relaxation time grows to values close to the thermalization time the hyperbolic oscillations are present for frequencies such that $\omega\tau \gg 1$.

For an approximation of first order in $(\omega\tau)^{-1}$, it is obtained that the maximum and minimum values of the amplitude are equal to those found in the foregoing case [Eqs. (26a) and (26b)] but the maxima are located in frequencies where the minima were, and vice versa. Similar conclusions are obtained for the maxima and minima of the phase [Eqs. (28) and (29)].

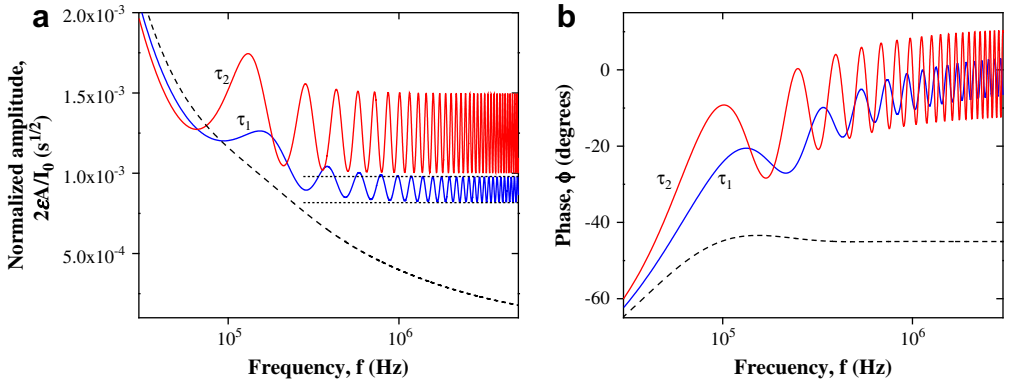

Fig. 4. Frequency dependence at $x = 0$ of the (a) normalized amplitude and (b) phase of the temperature for Neumann problem, when $\varepsilon_0/\varepsilon = 0$. The dashed lines correspond to the parabolic model and the solid lines to the hyperbolic model for two values of τ:$\tau_1 = 8\times10^{-7}$ s and $\tau_2 = 1.5\times10^{-6}$ s.

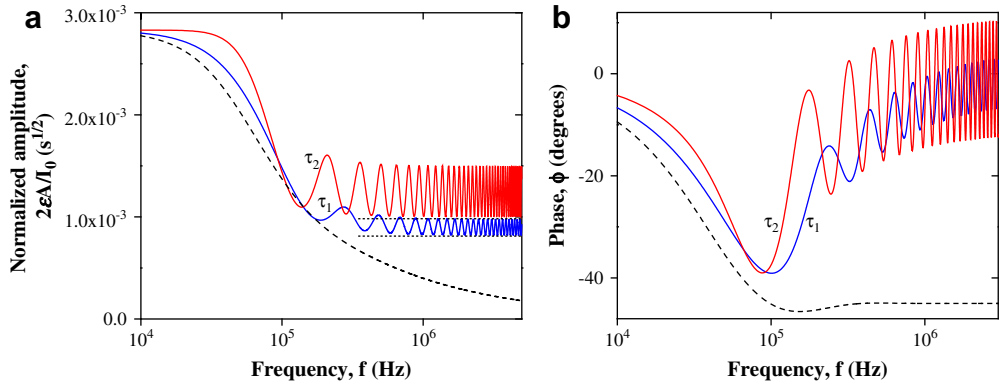

Fig. 5. Frequency dependence at $x = 0$ of the (a) normalized amplitude and (b) phase of the temperature, for Neumann problem, when $\varepsilon_0/\varepsilon \to \infty$. The dashed line corresponds to the parabolic model and the solid lines to the hyperbolic model for two values of τ:$\tau_1 = 8 \times 10^{-7}$ s and $\tau_2 = 1.5 \times 10^{-6}$ s.

3.2.3. Semi-infinite and finite layers with close thermal relaxation times: $\tau_0 = \tau + \Delta\tau$

Considering that $|\Delta\tau|/\tau \ll 1$ and $\omega\tau \gg 1$, for a first order approximation in $|\Delta\tau|/\tau \ll 1$ and $(\omega\tau)^{-1}$, the amplitude and phase spectra given in Eq. (13) are:

$$A(f) = \frac{I_0\sqrt{\tau}}{2\varepsilon}\sqrt{\frac{\left(e^{a/2}+Xe^{-a/2}\right)^2-4X\sin^2(\omega\tau a)}{\left(e^{a/2}-Xe^{-a/2}\right)^2+4X\sin^2(\omega\tau a)}}, \tag{32}$$

$$\phi(f) = -\frac{\pi}{4}+\frac{1}{2}\arctan(\omega\tau)+\arctan\left[\frac{2X\sin(2\omega\tau a)}{e^a-X^2e^{-a}}\right], \tag{33}$$

where X and a are defined in Eq. (20). The normalized amplitude and phase of the temperature are shown in Fig. 6(a) and (b) respectively, for the same data used in Fig. 4(a) and considering that $\varepsilon_0/\varepsilon = 0.5$ and $\Delta\tau = 5 \times 10^{-5}$ s. The corresponding amplitude and phase predicted by the parabolic model $\tau = 0$ are shown in the same figures by dashed lines. The hyperbolic model predicts again an oscillatory amplitude and phase at high frequencies ($\omega\tau \gg 1$).

Assuming that $X > 0$ it is obtained that the maximum and minimum values of the amplitude and phase:

■ For the amplitude [Eq. (32)], they are given by:

$$A_{\max} = \frac{I_0\sqrt{\tau}}{2\varepsilon}\frac{e^{a/2}+Xe^{-a/2}}{e^{a/2}-Xe^{-a/2}}, \tag{34a}$$

$$A_{\min} = \frac{I_0\sqrt{\tau}}{2\varepsilon}\frac{e^{a/2}-Xe^{-a/2}}{e^{a/2}+Xe^{-a/2}}. \tag{34b}$$

These extreme values of the amplitude occur at the frequencies given by Eq. (18), with the label "max" and "min" interchanged, which can be used to measure the thermal relaxation time τ, with Method 1. Solving Eqs. (34a) and (34b) for X, it is obtained:

$$X = \begin{cases} \left(\frac{a_{\max}-1}{a_{\max}+1}\right)e^a, & a_{\max} = \frac{2\varepsilon}{I_0\sqrt{\tau}}A_{\max}, \\ \left(\frac{1-a_{\min}}{1+a_{\min}}\right)e^a, & a_{\min} = \frac{2\varepsilon}{I_0\sqrt{\tau}}A_{\min}. \end{cases} \tag{35}$$

After having calculated τ and therefore the value of $a = l/\sqrt{\alpha\tau}$, using Eq. (35), X can be determined using the Method 2 and finally with Eq. (20), the value of $\Delta\tau$ can be measured.

■ For the phase [Eq. (33)], the maxima and minima are given by:

$$\phi_{\max} = -\frac{\pi}{4}+\frac{1}{2}\arctan\left[\left(n+\frac{1}{4}\right)\frac{\pi}{a}\right]+\arctan\left[\frac{2X}{e^a-X^2e^{-a}}\right], \tag{36a}$$

$$\phi_{\min} = -\frac{\pi}{4}+\frac{1}{2}\arctan\left[\left(n-\frac{1}{4}\right)\frac{\pi}{a}\right]-\arctan\left[\frac{2X}{e^a-X^2e^{-a}}\right], \tag{36b}$$

which occur at the frequencies given in Eq. (28) with the labels "max" and "min" interchanged and $n = 1,2,3,\ldots$. In this way, it is also possible to determine the thermal relaxation time τ with the

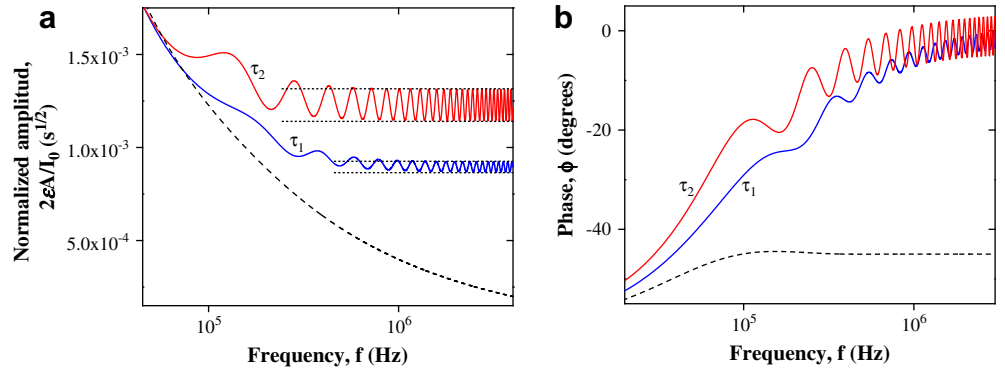

Fig. 6. Frequency dependence at $x = 0$ of the (a) normalized amplitude and (b) phase of the temperature, for Neumann problem, when $\tau_0 = \tau + \Delta\tau$. The dashed line corresponds to the parabolic model and the solid lines to the hyperbolic one for two values of τ:$\tau_1 = 8 \times 10^{-7}$ s and $\tau_2 = 1.5 \times 10^{-6}$ s with $\varepsilon_0/\varepsilon = 0.5$ and $\Delta\tau = 5 \times 10^{-5}$ s.

help of Eq. (28). Using Eqs. (36a) and (36b), the quantity X is obtained and therefore $\Delta\tau$ can be determined with Eq. (20).

Following a similar procedure for the temperature $\theta(x=l)$ (transmission configuration) than the one performed for $\theta(x=l)$ (reflexion configuration), it can be shown that at $x=l$ only the amplitude of the temperature presents an oscillatory behavior. This behavior of the amplitude can also be used for measuring the thermal relaxation time τ with a transmission configuration. These results are similar to those found for the Dirichlet problem.

In the Neumann problem, the reflexion configuration presents two advantages with respect to the transmission one; the first is that, it is possible to measure the thermal relaxation time using the amplitude as well as the phase. The second is that, the oscillation amplitudes observed at $x=0$ are much larger and therefore easier to observe than the oscillation amplitudes at $x=l$.

3.3. Simultaneous measurement of thermal properties

It is important to mention that up to this point, our approach for the determination of the thermal relaxation time has been based on the assumption that some of the thermal properties, such as the thermal diffusivity or thermal effusivity, of the materials are known. In homogeneous material, such as the individual layers analyzed in this work, measurements in the range of low modulation frequencies, using the parabolic approach, provide the value of the thermal diffusivity and thermal effusivity of the material [27,33], which can be used in the regime of high frequencies, where the hyperbolic effects are dominant, for the determination of the thermal relaxation time. However, it has been suggested that in order to determine the thermal relaxation time, it is important to measure the thermal diffusivity using a hyperbolic approach [18]. This is the situation for non-homogeneous materials with a complex structure, in which the effective thermal diffusivity of the material could depend on the modulation frequency [34]. Therefore, it is crucial, in this type of materials, to establish the thermal regime in which the experiments are performed and only the simultaneous determination of some thermal properties and of thermal relaxation time using the same heat transport model is adequate [18]. In our approach, for some of the analyzed configurations, it is possible to perform a simultaneous determination of the thermal properties. The cases in which this is possible are the following:

3.3.1. For the Dirichlet problem with $\varepsilon_0/\varepsilon = 0$ and when the monitoring of the temperature is performed at $x = l$ the difference in frequency for two successive maxima (minima) is (see [Eq. (18)])

$$\Delta f \equiv f_{n+1} - f_n = \frac{1}{2l}\sqrt{\frac{\alpha}{\tau}}. \tag{37}$$

The ratio of the maximum and minimum amplitudes is (from Eqs. (17)):

$$\Omega \equiv \frac{A_{\max}}{A_{\min}} = \coth(a/2), \tag{38}$$

where $a = l\sqrt{a\tau}$. Combining Eqs. (37) and (38), it is obtained that the thermal relaxation time and thermal diffusivity of the finite layer can be determined from:

$$\tau = \frac{1}{2\Delta f \ln\left(\frac{\Omega+1}{\Omega-1}\right)}. \tag{39}$$

$$\alpha = \frac{2l^2\Delta f}{\ln\left(\frac{\Omega+1}{\Omega-1}\right)}. \tag{40}$$

3.3.2. For the Neumann problem, when $\varepsilon_0/\varepsilon = 0$ and the measurement is performed at $x = 0$, the difference in frequency for two successive minima or maxima of the amplitude and phase [see Eqs. (18) and (28)] is also given by Eq. (37)

- From Eq. (26), the ratio between a maximum and a minimum of the amplitude is:

$$\Omega = \coth^2(a/2). \tag{41}$$

Combining Eqs. (37) and (41), it is obtained that

$$\tau = \frac{1}{2\Delta f \ln\left(\frac{\sqrt{\Omega}+1}{\sqrt{\Omega}-1}\right)}. \tag{42}$$

$$\alpha = \frac{2l^2\Delta f}{\ln\left(\frac{\sqrt{\Omega}+1}{\sqrt{\Omega}-1}\right)}. \tag{43}$$

In this case, Eq. (26) can be used to additionally determine the thermal effusivity of the first layer as follows:

$$\varepsilon = \frac{I_0}{2}\frac{\sqrt{\tau}}{\sqrt{A_{\max}A_{\min}}}, \tag{44}$$

and with $k = \varepsilon\sqrt{\alpha}$, its thermal conductivity can be obtained too. In this case four thermal properties can be determined by only performing an adequate frequency scan. It is important to mention that Eq. (44) is not only valid when $\varepsilon_0/\varepsilon = 0$ but also for any value of this ratio, in the regime of high frequencies ($\omega\tau \gg 1$).

- For the Neumann case, it is also possible to determine the thermal properties from the phase oscillatory behavior. From Eq. (29) it is known that the difference between a maximum and a minimum of the phase, when $n \gg 1/4$, is given by,

$$\Delta\phi \equiv \phi_{\max}(n) - \phi_{\min}(n) = 2\arctan\left[\frac{1}{\sinh(a)}\right]. \tag{45}$$

From Eqs. (37) and (45) it is obtained that two thermal properties are given by,

$$\tau = \frac{1}{2\Delta f \ln\left(\cot\left(\frac{\Delta\phi}{4}\right)\right)}. \tag{46}$$

$$\alpha = \frac{2l^2\Delta f}{\ln\left(\cot\left(\frac{\Delta\phi}{4}\right)\right)}. \tag{47}$$

Analogous results can be obtained for Neumann problem at $x=l$, however as mentioned before, higher values of the amplitude of the oscillations are obtained at $x=0$, therefore for such boundary conditions, the reflexion configuration is more convenient for the determination of the thermal properties. Similar results can also be obtained for the case $\varepsilon_0/\varepsilon = \infty$.

Based on these results, it can be concluded that our methodology would be useful to characterize not only homogeneous materials but also complex materials which thermal properties could depend on the frequency, being the simultaneous measurement of the thermal properties crucial. For these materials the reflexion configuration in which Neumann boundary conditions are fulfilled is the most adequate [18].

In order to evaluate how restrictive the conditions for the thermal effusivity in the presented methodology are, namely $\varepsilon_0/$

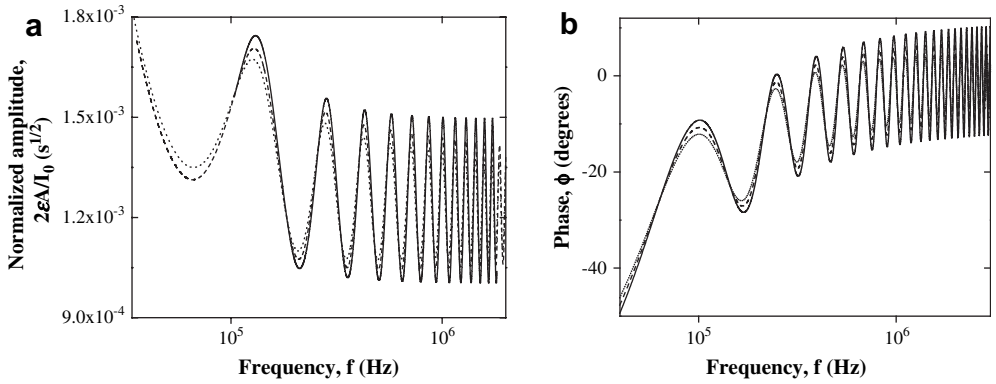

Fig. 7. Frequency dependence at $x = 0$ of the (a) normalized amplitude and (b) phase of the hyperbolic temperature, for Neumann problem. The solid, dashed and dotted lines correspond to $\varepsilon_0/\varepsilon = 0$, $\varepsilon_0/\varepsilon = 0.05$ and $\varepsilon_0/\varepsilon = 0.1$ respectively. Calculations were made using $\tau = 1.5 \times 10^{-6}$ s, $\tau_0 = 1.0 \times 10^{-7}$ s, $l = 20$ μm and $\alpha = 5 \times 10^{-5}$ m^2/s.

$\varepsilon = 0$ and $\varepsilon/\varepsilon;_0 = 0$, the study of the thermal profiles for the specific case in which $\varepsilon_0/\varepsilon \ll 1$ was done. In Fig. 7(a) and (b), the spatial part of the amplitude and phase of the surface temperature respectively, are depicted as a function of the frequency for three different values of the quotient $\varepsilon_0/\varepsilon$ of the thermal effusivities.

It is shown that even though for relatively high ratios as $\varepsilon_0/\varepsilon = 0.1$, the minima and maxima appear nearly at the same frequencies and that the values of those extremes do not vary significantly. In fact for the third maxima ($n = 3$), $f = 4.33 \times 105$ Hz and the curve that belongs to the case $\varepsilon/\varepsilon_0 = 0$, it only differs by 3.6% and 6.9% with respect to the curves of the cases $\varepsilon_0/\varepsilon = 0.05$ and $\varepsilon_0/\varepsilon = 0.01$, respectively. These ratios of thermal effusivities can be fulfilled by common materials [27]. Of course for higher values of the ratio of thermal effusivities ($\varepsilon_0/\varepsilon$), our analytical formulas are not convenient (unless $\varepsilon_0/\varepsilon \gg 1$) [see Eqs. (30) and (31)], but the general approach is. In these situations more complex procedures must be used and the highly structured thermal profiles can be expected to cast successful results.

It is important to mention that the presented methodology is useful when the interface thermal resistance is sufficiently small to be neglected. Our approach considers that when the thermal effusivities of the layers are quite different or their thermal relaxation times are similar, the amplitude and phase of the spatial part of the oscillatory surface temperature must be independent of the thermal properties of the semi-infinite layer. If the interface thermal resistance is considered, the contribution of the thermal relaxation time τ_0, due to the semi-infinite layer cannot be neglected. Therefore the presented methodology would not be applicable. In this sense our approach is a first approximation to the real problem and constitutes a limiting case of a more general formulation for the thermal relaxation time determination.

4. Conclusions

In this work the heat transport governed by the Cattaneo–Vernotte hyperbolic equation in a system formed by a finite layer in thermal contact with a semi-infinite layer when a periodic heat source is applied to the first one is considered. It has been shown that remarkable oscillations of the amplitude and phase of the spatial component of the surface temperature are obtained in the high frequency regime for Dirichlet and Neumann boundary conditions. The observation, in an experiment of these oscillations would constitute an unmistakable characteristic of hyperbolic behavior. Furthermore it has been shown that the analysis of the oscillation is useful in the determination of the thermal relaxation time for homogeneous layers using simple analytical formulas when the thermal effusivities of the layers are quite different or their thermal relaxation times are similar. Additionally, it has been shown that our approach is useful in such cases in which it is necessary to determine simultaneously the thermal properties of a material in a range of modulation frequencies. It has also been shown that the approximations performed for obtaining the analytical formulas for the extremes are not too restrictive but that they can be fulfilled by common materials. This work could be used as the basis for heat transport models which can take into account the interface thermal resistance between adjacent layers. Our approach, in which the interface thermal resistance is neglected, constitutes a limiting case of a more general formulation for the thermal relaxation time determination.

References

[1] H.S. Carslaw, J.C. Jaeger, Conduction of Heat in Solids, second ed. Oxford University Press, London, 1959.
[2] A.N. Tikhonov, A.A. Samarskii, Equations of Mathematical Physics, Dover Books on Physics and Chemistry New York (1990).
[3] D.D. Joseph, L. Preziosi, Heat waves, Rev. Mod. Phys. 61 (1) (1989) 41–73.
[4] D.Y. Tzou, A unified field approach for heat conduction from macro- to micro-scales, J. Heat Transfer 117 (1) (1995) 8–16.
[5] J.P. Mckelvey, Solid State and Semiconductor Physics, Harper & Row, New York, 1966.
[6] Jing Liu, Xu Chen, X. LisaXu, New thermal wave aspects on burn evaluation of skin subjected to instantaneous heating, IEEE Trans. Biomed. Eng. 46 (4) (1999) 420–428.
[7] B. Diatta, C. Wafo Soh, C.M. Khalique, Approximate symmetries and solutions of the hyperbolic heat equation, Appl. Math. Comput. 205 (1) (2008) 263–272.
[8] Tzu-Ching Shih, Hong-Sen Kou, Chihng-Tsung Liauh, Win-Li Lin, The impact of thermal wave characteristics on thermal dose distribution during thermal therapy: a numerical study, Med. Phys. 32 (9) (2005) 3029–3036.
[9] C. Cattaneo, Sulla coduzione del calone, Atti. Semin. Mat. Fis. Univ. Modena 3 (1948) 83.
[10] P. Vernotte, Les Paradoxes de la Theorie Continue de l'equation de la Chaleur, C.R. Acad. Sci. 246 (22) (1958) 3154–3155.
[11] S. Galovic, D. Kotoski, Photothermal wave propagation in media with thermal memory, J. Appl. Phys. 93 (5) (2003) 3063–3070.
[12] A.E. Kronberg, A.H. Benneker, K.R. Westerterp, Notes on wave theory in heat conduction: a new boundary condition, Int. J. Heat Mass Transfer 41 (1) (1998) 127–137.
[13] P.J. Antaki, Analysis of hyperbolic heat conduction in a semi-infinite slab with surface convection, Int. J. Heat Mass Transfer 40 (13) (1997) 3247–3250.
[14] A. Vedavarz, S. Kumar, M.K. Moallemi, Significance of non-Fourier heat waves in conduction, ASME J. Heat Transfer 116 (1) (1994) 221–224.
[15] M.N. Ozisik, D.Y. Tzou, On the wave theory in heat conduction, ASME J. Heat Transfer 116 (3) (1994) 526–535.
[16] W. Kaminski, Hyperbolic heat conduction equation for materials with a non-homogeneous inner structure, ASME J. Heat Transfer 112 (3) (1990) 555–560.
[17] K. Mitra, S. Kumar, A. Vedavarz, M.K. Moallemi, Experimental evidence of hyperbolic heat conduction in processed meat, ASME J. Heat Transfer 117 (3) (1995) 568–573.
[18] W. Roetzel, N. Putra, K. SaritDas, Experiment and analysis for non-Fourier conduction in materials with non-homogeneous inner structure, Int. J. Therm. Sci. 42 (6) (2003) 541–552.

[19] L. Wang, X. Zhou, X. Wei, Heat Conduction: Mathematical Models and Analytical Solutions, Springer-Verlag, Berlin, Heidelberg, 2008.
[20] A. Graßmann, F. Peters, Experimental investigation of heat conduction in wet sand, Heat Mass Transfer 35 (4) (1999) 568–573.
[21] H. Herwig, K. Beckert, Experimental evidence about the controversy concerning Fourier or non-Fourier heat conduction in materials with a nonhomogeneous inner structure, Heat Mass Transfer 36 (5) (2000) 387–392.
[22] Y. Mengi, D. Turhan, The influence of retardation time of the heat flux on pulse propagation, J. Appl. Mech. 45 (1978) 433–435.
[23] Zhi-Ming Tan, Wen-Jei Yang, Heat transfer during asymmetrical collision of thermal waves in a thin film, Int. J. Heat Mass Transfer 40 (17) (1997) 3999–4006.
[24] A.F. Khadrawi, M.A. Al-Nimr, M. Hammad, Thermal behavior of perfect and imperfect contact composite slabs under the effect of the hyperbolic heat conduction model, Int. J. Thermophys. 23 (2) (2002) 581–598.
[25] F.A. Mcdonald, G.C. Westel Jr., Generalized theory of the photoacoustic effect, J. Appl. Phys. 49 (4) (1978) 2313–2322.
[26] J.L. Pichardo, J.J. Alvarado-Gil, Open photoacoustic cell determination of the thermal interface resistance in two layer systems, J. Appl. Phys. 89 (7) (2001) 4070–4075.
[27] D.P. Almond, P.M. Patel, Photothermal Science and Techniques, Chapman & Hall, London, 1996.
[28] A. Salazar, A. Sánchez-Lavega, J.M. Terrón, Effective thermal diffusivity of layered materials measured by modulated photothermal techniques, J. Appl. Phys. 84 (6) (1998) 3031–3041.
[29] W.P. Leung, A.C. Tam, Techniques of flash radiometry, J. Appl. Phys. 56 (1) (1984) 153–161.
[30] P. Guillemet, Jean-Pierre Bardon, Conduction de la chaleur aux temps courts: les limites spatio-temporelles des modèles parabolique et hyperbolique, Int. J. Heat Mass Transfer 39 (9) (2000) 968–982.
[31] A. Mandelis, Diffusion Waves Fields: Mathematical Methods and Green Functions, Springer, New York, 2001.
[32] A. Rosencwaig, A. Gersho, Theory of the photoacoustic effect with solids, J. Appl. Phys. 47 (1) (1976) 64–69.
[33] H. Vargas, L.C.M. Miranda, Photoacoustic and related photothermal techniques, Phys. Rep. 161 (2) (1988) 43–101.
[34] J.L. Lucio, J.J. Alvarado-Gil, O. Zelaya-Angel, H. Vargas, On the thermal properties of a two-layer system, Phys. Status Solidi (a) 150 (2) (1995) 695–704.